SINGLE-WALL CARBON NANOTUBE FILMS COATING BY DIP-COLLOIDAL NANOCRYSTALS BILAYER FILMS

A Thesis
Submitted to the Graduate Faculty
of the
North Dakota State University
of Agriculture and Applied Science

By

Amal Ahmed Altayyar

In Partial Fulfillment of the Requirements
for the Degree of
MASTER OF SCIENCE

Major Program:
Materials and Nanotechnology

October 2019

Fargo, North Dakota

NORTH DAKOTA STATE UNIVERSITY

Graduate School

Title

SINGLE-WALL CARBON NANOTUBE FILMS COATING BY DIP-COLLOIDAL NANOCRYSTALS BILAYER FILMS

By

Amal Ahmed Altayyar

The supervisory committee certifies that this thesis complies with North Dakota State University's regulations and meets the accepted standards for the degree of

MASTER OF SCIENCE

SUPERVISORY COMMITTEE:

Dr. Erik Hobbie
Chair

Dr. Yongki Choi

Dr. Danling Wang

Approved:

November 13, 2019
Date

Dr. Erik Hobbie
Department Chair

ABSTRACT

A wrinkling approach was used to study the mechanics of hybrid nanotube/nanocrystal coatings adhering to soft polymer (PDMS) substrates. We focused on three thicknesses: 10 nm, 30 nm, and 40 nm. The approach we used is the Strain-Induced Elastic Buckling Instability for Mechanical Measurements (SIEBIFMM) technique, which allows measurement of the SWCNT film mechanics by the buckling wavelength and the film thickness by inducing a compressive stress in the films at different strains; 2%, 4%, 6%, 8%, 10%, and 12%. In this thesis, dip-coating method with colloidal nanocrystals was used to enhance the rigidity of the carbon nanotube films by filling the pores of the nanotube network. Our results show an almost two-fold enhancement in the Young modulus of a thin SWCNT film related to the presence of a thin interpenetrating over-layer of the semiconductor nanocrystal.

ACKNOWLEDGEMENTS

I would like to show my gratitude to Professor Erik Hobbie who has cheerfully answered my queries and given me good guidelines for research throughout numerous consultations,as well as provided me with materials. He is always a supportive and optimistic person. I would also like to expand my deepest gratitude to all those who have directly and indirectly guided me in writing this thesis: Abdullah Altayyar, Reema Altayyar,and especially Mohammed Alziyadi assisted me in a myriad way with the writing and helpfully comments on earlier drafts of this thesis.

A big thank you to Professor Yongki Choi and Professor Danling Wang for being willing a part of the committee for my Master's Thesis, as well.

Finally, I do not want to forget to thank my friends for their lasting support throughout the production of this research: Meshal Alzaid, Eid Almutairi, and Salim Thomas.

DEDICATION

To my parents for making me who I am, and to my sweetheart husband and my little son for supporting me all the way.

TABLE OF CONTENTS

LIST OF TABLES

LIST OF FIGURES

1. INTRODUCTION

1.1. Flexible Electronics

Flexible electronics has attracted attention in recent years for many applications, such as solar cells, biosensors, wireless power, and signal transmission sheets, e-skin, e-paper, and flexible display [1]. Flexible electronics is a new trend in the world of electronics. It has characteristics which conventional electronics do not have. It is true that most of our electronics are currently conventional electronics, for example, cell phones, televisions, computer displays, and medical equipment screens. However, these are considered rigid materials, which suffer from cracks and failure when they are bent, twisted, or faced with mechanical trauma [2]. Also, conventional electronics have limits on cost and hardness. For example, Indium Tin Oxide (ITO) is a ternary composition of indium, tin, and oxygen in varying proportions. Indium tin oxide is one of the most widely used materials in electronics because of its two main properties: optical transparency and electrical conductivity [3]. However, despite ITO's strengths, ITO is fragile, the quantity is limited, and it has limited mechanical flexibility. So, we must discover another alternative. Flexible electronics can provide high mechanical flexibility and low weight using solution processes and low-cost materials.

Many potential applications have been explored, including displays, computational systems, energy storage and generation systems, health care,and e-textiles. Flexibility in electronic materials is also desirable for biomedical engineering and bioengineering,with the potential to be integrated into the human body.Humidity, heat,and pressure sensor arrays,for example, might be incorporated into a bed sheet and watch a patient in real time. These kinds of devices could be used in other areas as well, such as military and defense applications. Soldiers would not need to carry bulky devices in the field as these could be incorporated into their uniforms to make it easy and fast for them to provide and access such data [4]. Also, intelligent roads could be engineered with the aim of improving road safety, lowering road congestion, and lowering energy consumption. The road and car would also be able to interact dynamically, by adjusting either party to optimize their systems energetically [4].

Moreover, flexible electronics have a high possibility to be used in photovoltaic panels. People could roll up and clean their solar panels easily, rather than relying on rigid silicon panels, which are brittle and heavy [2]. To achieve this it could be beneficial to use SWCNT thin films.

1.2. Carbon Nanotubes (CNTs)

1.2.1. Structure

Carbon nanotubes can be conceptualized as thin sheets of graphite or graphene that have rolled into a tube.They were discovered in 1991 by Sumio Iijima [5]. A graphene sheet can be rolled up in more than one way, producing different types of CNTs [5]. CNTs are considered one-dimensional structures, and they have a diameter of roughly 1 nm and an aspect ratio (length divided by width) of up to 1000. Most essential structures are single-walled carbon nanotubes (SWCNTs) and multi-walled carbon nanotubes (MWCNTs) Figure 1.1 (a). For MWCNTs, the concentric cylinders have a radial spacing of 0.34 nm, which is close to the inter-plane spacing of graphite [6]. In this thesis, SWCNTs will be considered because the properties of SWCNTs are better compared to MWCNTs. In general, the bonding in CNTs is sp^2, consists of honeycomb lattices. CNTs are seamless structures, with each atom joined to three neighbors, as in graphite. So, the tubes can be considered to be rolled-up graphene sheets (SWCNTs) with diameters that range from 0.3 nm to 3 nm and lengths up to millimeters [6]. Also, SWCNTs can be either metallic or semiconducting, which expands their area of applications. This variety is due to the wrapping of a graphene sheet, which is described by the chiral vector $c = na_1 + ma_2$, where: n and m are integers, and a_1 and a_2 are the unit cell vectors of the two-dimensional lattice formed by the graphene sheets. For example, to produce a CNT with the indices (6,3),the sheet is rolled up so that the atom labeled (0,0) is superimposed on the one labeled (6,3) [7]. Carbon nanotubes are only described by the pair of integers (n, m) which is related to the chiral vector. So, when the chiral angle is $0^\circ < \theta < 30^\circ$ and the chiral indices are not equal ($n \neq m$), the SWCNT is called "chiral", and when the chiral angle is 30°, and the chiral indices are equal (n=m), the SWCNT is called "armchair". Finally, when the chiral angle is 0°, and one of the chiral indices is zero $(n, 0)$ or $(0, m)$, the SWCNT is called "zig-zag". The chirality of the SWCNT determines many properties, but primarily the diameter and the band structure or electronic type Figure 1.1 (b) [8, 9].

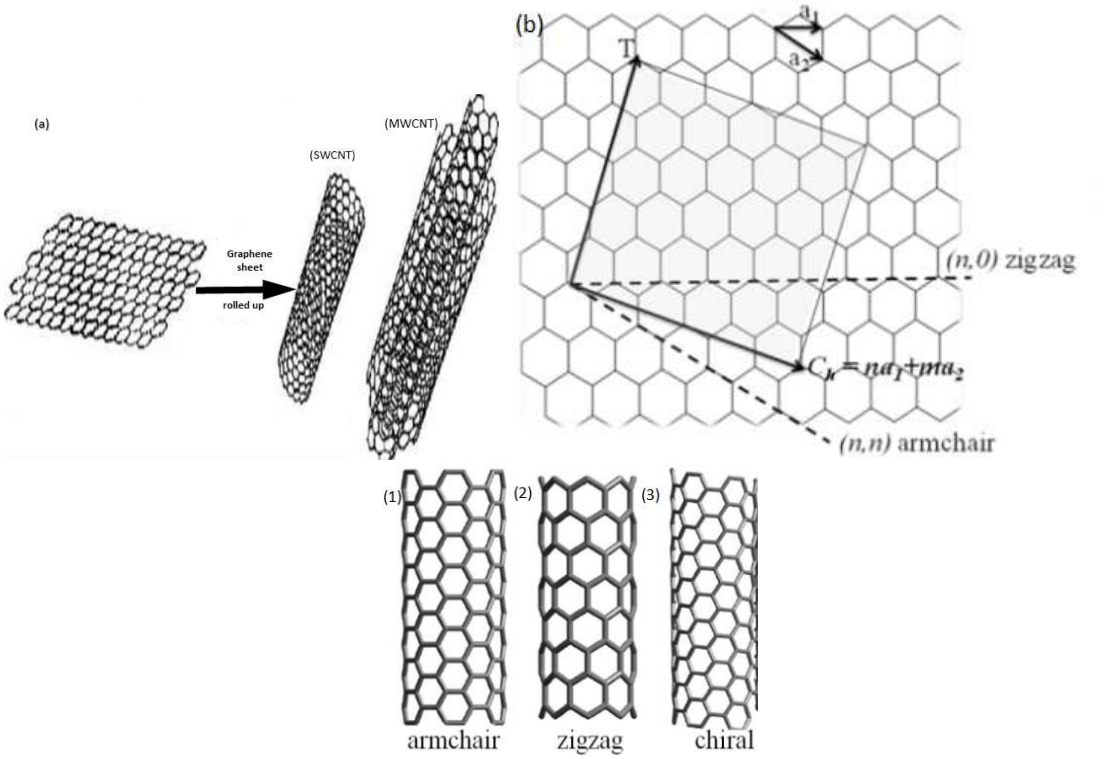

Figure 1.1. (a) A sheet of graphene rolled to show SWCNT and MWCNT.The difference in structure is easily seen at the open end of the tubes.(b) Chiral vector with (1) armchair structure, (2) zig-zag structure, and (3) general chiral structure [11].

1.2.2. Synthesis

The electric arc discharge technique was used in the early sixties by R. Bacon for the synthesis of carbon fibers. It is the oldest method for carbon nanotube production. In 1990 the same process was adopted by Huffman and Krätschmer to produce fullerenes, later it was improved and applied for the synthesis of multi wall carbon nanotubes (MWCNTs) and single wall (SWCNTs) carbon nanotubes [9]. Other methods to produce carbon nanotube are the laser ablation and chemical vapor deposition (CVD) [10]. The laser ablation process is technically like the arc discharge method. The difference between these two methods is in the quality and purity of the obtained products. However, the arc discharge and the different types of CVD are the most utilized techniques for the production of carbon nanotubes.

1.2.2.1. Arc Discharge Method

Arc discharge method was discovered by Ebbesenand Ajayan, NEC, Japan 1992 [10]. The arc discharge technique employs the use of two purity graphite electrodes,and the anode and cathode are pure graphite as shown in Figure 1.2. The synthesis is executed at low pressure (30-130 torr or 500 torr) in a controlled atmosphere composed of inert or reactant gas and the flow of a current (50-150 A). The temperature in the inter-electrode area is so high that carbon sublimes from the positive electrode or "anode". From the anode position, a fixed gap between the anode and the cathode is maintained. A plasma is formed between the electrodes. To get better results,bimetallic catalysts can be used [11,12]. When no incentive is used, only the soot and the deposit are formed. The residue contains fullerenes while MWCNTs, together with graphite carbon nanoparticles, are found in the carbon deposit. The outer diameter of the MWCNTs is in the range of 2–25 nm, and the tube length often exceed 1 μm. Also, the SWCNTs have diameters of 1.1–1.4 nm. When metal catalysts are evaporated with carbon in the arc discharge, the essence of the deposit has MWCNTs, and SWCNTs .The physical and chemical factors that influence the arc discharge method are the carbon vapor dispersion in inert gas, the carbon vapor concentration, the temperature, and the composition of the catalyst. These factors affect the type of nanotubes, the growth of the nanotubes, and their inner and outer diameters [13].

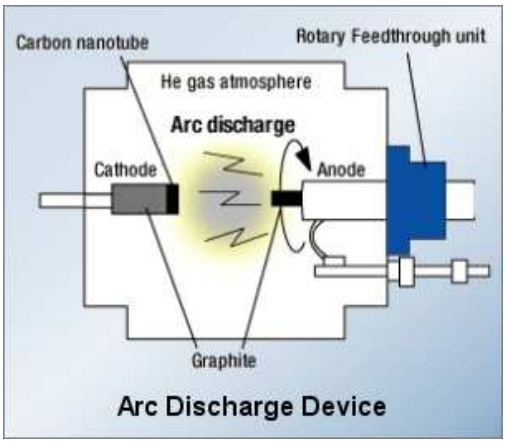

Figure 1.2. Schematic representation of arc discharge apparatus [11, 12].

1.2.2.2. Laser Ablation Method

The laser ablation process to produce single-wall carbon nanotubes (SWCNTs) was developed by Guo et al. at Rice University [14]. In 1995, Smalley et al. developed a laser ablation method to produce SWCNTs [15]. In general, the production of SWCNTs though the laser ablation method is better than the production of SWCNTs through the arc discharge method. Guo's group used the oven laser-vaporization apparatus, which used to produce fullerenes, multi-walled nanotubes, and metallofullerenes [16]. A laser beam of 532 nm was focused on a graphite composite target at 1200°C. Flowing Ar gas sweeps the soot produced by the laser vaporization from the high-temperature zone and deposits it onto water-cooled copper Figure 1.3. At room temperature, a paste produced from mixing high-purity metal was placed in a form. The frame was placed in a hydraulic press equipped with heating plates at 130°C for four-five hours under constant pressure. It was baked at 810°C for eight hours. Subsequent runs with this step were made after two hours heating at 1200°C, to control the quality and quantity by the type of metal catalysts and their ratio [17–19], the kind of the gas and its pressure [20–22], the temperature [23–25], and the laser parameters [26–28].

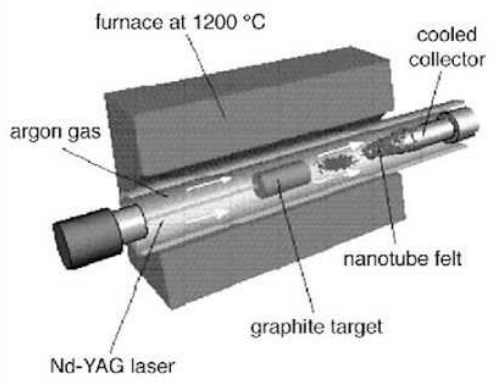

Figure 1.3. Laser ablation technique [17].

1.2.2.3. Chemical Vapor Deposition Method

Chemical vapor deposition (CVD) is used for the production of nanotubes with excellent properties [29]. Yacamàn et al. were the first to use this technique to produce carbon nanotubes [30]. Today, the chemical vapor deposition (CVD) method is considered to be the only economically

viable process for large-scale CNTs production [31]. This method is not as expensive as the previous two methods and has the potential to be used widely in industry. Also, it has other advantages, such as low power input and low-temperature conditions. However, the produced CNTs do not have high purity due to impurities from the metal substrate and the catalyst [8]. In principle, chemical vapor deposition (CVD) is the catalytic decomposition of hydrocarbon feedstock with the aid of supported transition metal catalysts Figure 1.4. Generally, the experiment was done in the oven under atmospheric pressure. The catalyst was placed in a ceramic boat which was put into a quartz tube. Then, the mixture containing an inert gas and hydrocarbon was passed over the catalyst bed at temperatures ranging from 500°C to 1100°C. The system is then cooled down to room temperature. The carbon and catalyst are inoculated at the top of oven, and the filaments grow and are collected at the bottom. The supported catalyst is placed in the middle and an upward flow of carbon is used [32]. The general nanotube growth technique, in the (CVD) process, involves the dissociation of hydrocarbon molecules catalyzed by the transition metal and the saturation of carbon atoms in the metal nanoparticle. The precipitation of carbon from the metal particle leads to the formation of tubular carbon solids in a sp^2 structure. By changing the active particles on the surface of the catalyst, nanotube diameter can be controlled, and the length of the tubes can also be controlled by reaction time; even up to 60 mm long tubes can be produced [33].

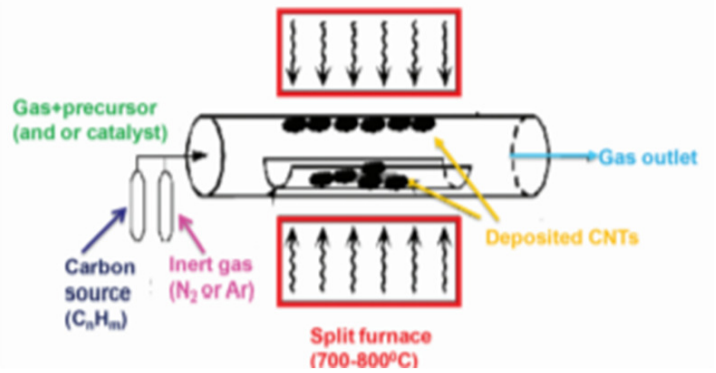

Figure 1.4. Chemical vapor deposition technique [32].

1.2.3. Properties

CNTs are composed of pure carbon, therefore,they exhibit high electrical conductivity, high stability, and environmental friendliness. Theoretically, a metallic nanotube can carry a current density that is more than 1000 times greater than metals such as copper. As well, SWCNTs have a thermal conductivity about 10 times higher than copper [34]. In a SWCNT, each C atom is bonded with three carbon atoms, which forms three sp^2 orbitals through hybridization. Also, SWCNTs have a high young modulus and tensile strength. This strength is imputed to the covalent sp^2 bonds between carbon atoms [35]. The Young modulus of SWCNT can be about 270 to 950 GPa, where the theoretical limit is up to 1.2 TPa.The tensile strength, where the material fails under stress, falls between 150 to 180 GPa [36]. A comparison of the Young modulus of individual CNTs with other materials can be made. For example, the Young modulus of CNTs is 650-1000 GPa, while the Young modulus of copper and steel are 130 GPa and 180 GPa respectively. In addition, SWCNTs have a lower density ($0.8 g/cm^3$) in comparison to other materials [37].

1.3. Nanocrystals (NCs)

The nanocrystal is a central theme in nanotechnology. Semiconductor nanocrystals are little crystalline particles that exhibit optical and electronic properties according to the size of the particles [38–40]. Therefore, when the size of the particle changes to the nanoscale, the features of the material change [41]. The nanocrystal typically has dimensions in the range of 1-100 nm. Nanocrystals have a wide variety of proven and potential applications because they have many unique optical and transport properties [42].

Bulk semiconductors have a composition-dependent band gap energy (E_g), which is the minimum energy required to excite an electron from a valence energy band into the vacant conduction energy band Figure 1.5. The exciton has a finite size within the crystal defined by the Bohr exciton diameter (a_B), which can vary from 1 nm to more than 100 nm, depending on the material. If the size of a semiconductor nanocrystal is smaller than the size of the exciton, the charge carriers become spatially confined, which raises their energy. Therefore, the exciton size delineates the transition between the regime of bulk crystal properties and the quantum confinement regime, in which the optical and electronic properties are dependent on the nanocrystal size. Nanocrystals

with dimensions smaller than (a_B) demonstrate size-dependent absorption and fluorescence spectra with discrete electronic transitions [43].

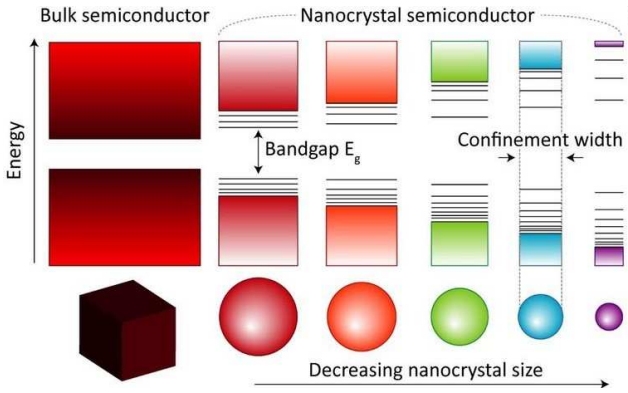

Figure 1.5. Electronic energy states of semiconductors crystals and bulk semiconductors [43].

1.4. SWCNT Films/ Colloidal Nanocrystals Composite

Thin films and coatings are used in a legion of technologies for a variety of purposes [44]. For some applications, such as touchscreen displays, solar cells, and light-emitting diodes, the electrical characteristics of the film are very important. So, the use of SWCNTs creates promising new opportunities and the potential for a large number of applications. Because SWCNTs have a high Young's modulus (1.2 TPa) and they have the same shape as polymer, they are appropriate for nanocomposite applications, although their full mechanical potential is not yet understood. A SWCNT thin film adhered to a soft substrate and compressed under weak strain shows a plastic response because of bundling between SWCNTs mediated by van der Walls interactions between individual nanotubes, which is also associated with small diameter, long length, and high aspect ratio [45].

In this regard, the microscopic distinct element method (mDEM) has been used to explore an excluded-volume approach to stabilizing SWCNT networks against strain-induced plastic change. The target of this is reducing the rearrangement of the SWCNT network in response to an applied strain by filling the porous structure with a second nanomaterial, for example, colloidal nanocrystals (NCs) [45, 46].

1.5. Research Approach

1.5.1. Fabrication Method

For SWCNT film fabrication, we used a vacuum filtration method to deposit the SWCNTs on a cellulose filter membrane. This method has many advantages. First, it is an exact process for producing SWCNT films with nanoscale thickness by control of the SWCNT concentration. Second, it can produce uniform films using surfactants and precursor solutions that have ideal SWCNT dispersion. Also, it is not an expensive method, and it does not need to use volatile solvents, relying instead on the water for the filtration process. At the end of the method, acetone is used to dissolve the cellulose filter paper and free the film. For coating fabrication, we used an approach different from the above-mentioned methods. We made an interface by applying a coating on the SWCNT film: one of the sides was SWCNT film with nanocrystals, and the other was SWCNT film without nanocrystals. We used this method because the SWCNT/CdSe NC bilayer geometry a simple structure that is easy to process and model. Also, in our method, we can produce homogeneous composites with a NC volume fraction that is small.

1.5.2. Characterization Technique

In this research, we used a strain-induced elastic buckling instability for mechanical measurement (SIEBIMM) technique to measure the mechanical properties of the thin nanocomposite films. When subjected to a compressive strain, the thin films adhered to elastomeric substrates, producing periodic wrinkles that are directly related to the mechanical properties of the film [47]. The periodic wrinkles have different length scales depending on the mechanical properties of the materials and the nature of the strain that induces the wrinkles. In particular, the wavelength (λ) of these periodic wrinkles can be used to understand the elasticity of the film [48]. The (SIEBIMM) technique has many advantages, such as being a simple and inexpensive method. Also, it offers advantages over nanoindentation because it avoids uncertainties associated with indentation depth and the proximity of the substrate. SIEBIMM is a linear model, and when applied to a homogeneous thin film, it predicts harmonic wrinkles. So, to extract Young's modulus of thin homogeneous films such as polymers we can use the SIEBIMM method. In contrast, SWCNT films produce disturbed wrinkles due to quenched fluctuations in SWCNT film thickness [49, 50]. However, the SIEBIMM method can be used for inhomogeneous films, such as SWCNT films. Since the earlier research,

Rogers and coworkers have measured the Young modulus of oriented individual SWCNTs on a PDMS substrate using this technique. For tubes with diameters of 1-3 nm, they got a SWCNT Young modulus of 1.3 TPa $\pm$ 0.2 TPa, which agrees with previous atomic-force microscopy (AFM) measurements [51]. The wrinkles in thin SWCNT films can be modeled through random thickness fluctuations [52,53]. The mechanical properties can be obtained by applying a strain to a thin film adhered to a soft elastic substrate, which, in our case, is PDMS. So, by characterizing the amplitude of the resulting wrinkles and the wavelength, we can extract information about the modulus of the film. Knowledge of the wrinkling wavelength, film thickness, the Poisson ratios and the Young modulus of the substrate are enough to get the elasticity of the film, through the following equation:

$$E_f = \left(\frac{\lambda}{2\pi h}\right)^3 \left(\frac{3E_s(1-v_f^2)}{(1-v_s^2)}\right) \tag{1.1}$$

Where λ is the wavelength of the harmonic wrinkles, h is the film thickness, and $\bar{E}_i = E_i/(1-v_i^2)$ is the plane-strain modulus, where i can denote the substrate ($i = s$) or the film ($i = f$), and v is the Poison ratio [54]. The method we used to image the wrinkled films is optical reflection microscopy. Also, to measure the thickness of the film, we used atomic force microscopy (AFM) and a broadband lamp for excitation and a spectrometer for light detection (for measuring thickness through optical absorption). To obtain the fundamental wrinkling wavelength, we used both direct counting and the two-point height-height correlation function $c(r) = \langle u(r)u(0)\rangle$ to extract the wrinkling wavelengths. The projection along the strain direction, $c(x)$, has peaks at $x = \lambda, 2\lambda$, or 4λ as shown in Figure 1.6 [54]. ImageJ was used to compute the correlation functions from threshold binary images, averaging together correlation results from four images, each 250 by 250 pixels in size [55,56].

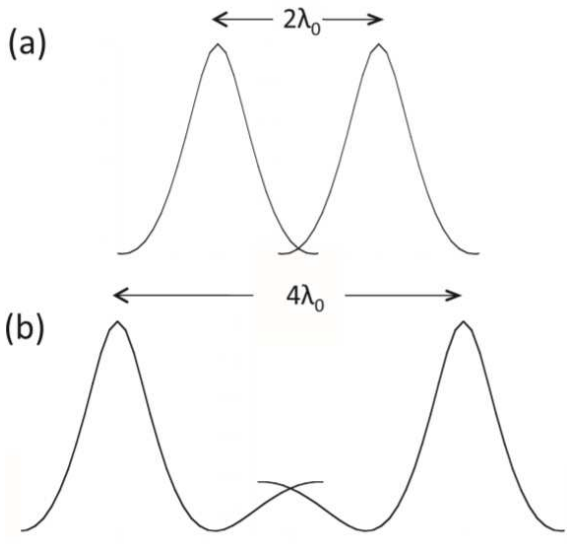

Figure 1.6. Schematic of bifurcation (a) 2λ, or (b) 4λ in an inhomogeneous film [53].

1.6. Objective

CNTs films are considered semi-porous structures with van der Walls attractions that are enhanced by large aspect ratios [37]. CNT interactions in the film are van der Walls attractions, which along with limited sliding friction, allows the CNTs to align in bundles in a direction perpendicular to the applied stress, leading to a phenomenon called strain softening. Strain softening decreases the rigidity of CNT films when they are compressed and can also affect electrical conductivity [57]. Hence, understanding the mechanical characteristics of CNTs in the thin film would be useful for applications such as flexible electronics. Our study focused on a mutual reinforcing mechanism, where not only the excellent properties of CNTs would support the nanocrystals, but the nanocrystals would decrease the strain-softening of the CNTs by filling the pores of the CNT network [45]. Previously, we explored coating or spraying the nanocrystals onto single-wall carbon nanotube (SWCNT) thin films. Examples of such fillers include nanocrystals (CdSeNCs, SiNCs), and poly (3,4ethylenedioxthiophene) poly (styrene sulfonate) (PEDOT: PSS) films. In this research, we used nanocrystals (CdSe NCs) as fillers for single-wall carbon nanotube (SWCNT) thin films. In addition, we used the wrinkling approach to study the mechanical properties of SWCNT with nanocrystals and without nanocrystals on a soft substrate by measuring the Young modulus

as a function of the layer thickness. Finally, we wanted to know the optimal layer thickness that would result in optimum behavior.

2. EXPERIMENTAL PROCEDURE

2.1. Sample Preparation

2.1.1. Single Wall Carbon Nanotubes Films

Vacuum filtration was used to produce SWCNT films with nanoscale thickness Figure 2.1. First, we soaked a 0.05 μm cellulose filter paper in deionized (DI) water with 5% ethanol in a petri dish for 2 hours. Every part of the vacuum filtration was washed with deionized water. Then, we placed the filter paper on the glass filter. Next, we put the glass filter on the flask and adjusted the level of the flask using a bubble level to avoid an unbalanced situation, which would lead to a concentration gradient in the film. After we assembled the components of the filtration system, we poured 200 ml of deionized water and mixed 20% ethanol with it inside the beaker and let it stabilize for 2 minutes to remove any bubbles. We prepared SWCNT films of different thickness by varying the SWCNT concentration. For example, to get a 40 nm film thickness, a volume of 15 μl of stock SWCNT solution (1% concentration) was taken by a pipette, checked to confirm there was no bubble in the pipette, and mixed 485 μl of deionized water in a clean vial to yield a total volume of 500 μl. Using the pipette, we slowly deposited the 500 μl solution on the center of the cellulose filter paper, which was placed on the glass filter, which helped to uniformly disperse the SWCNTs on the filter to produce a uniform surface coating. For a 20 nm SWCNT film, we took a volume of 18 μl SWCNT solution and mixed it with 493 μl while for 10 nm film, we took 7 μl of SWCNT solution and mixed it with 482 μl DI water. We let the solution equilibrate for 15 minutes before applying a vacuum. After applying the vacuum for 1 to 2 hours, all the solution was deposited through the filter paper and had a uniform film of SWCNT.

Figure 2.1. Vacuum filtration setup that we used in our project.

Then, we locked the vacuum and waited for 20 minutes until the surface was exposed, and then we removed the SWCNT filter paper assembly using tweezers. Figure 2.2 shows an example of the 20 nm film thickness.

Figure 2.2. 20 nm thick SWCNT film that was produced by Vacuum filtration

To get freestanding films, we cut one rectangle from the SWCNT film with a length 10 mm and a width of 2.64 mm. Then, we transferred it to a separate vial of acetone for 1 hour to dissolve the filter paper backing. After 1 hour, we transferred it again to another acetone vial for another hour. The purpose of the first acetone vial was to dissolve most of the filter paper, while the purpose of the second vial was to make sure all the filter paper dissolved. Then, we transferred the freestanding film to an ethanol vial for 24 hours to ensure the removal of any residual surfactants still in the SWCNT film Figure 2.3 (a). The transferring method is unique and was developed in our laboratory by collecting the SWCNT film with a pipette Figure 2.3 (b).

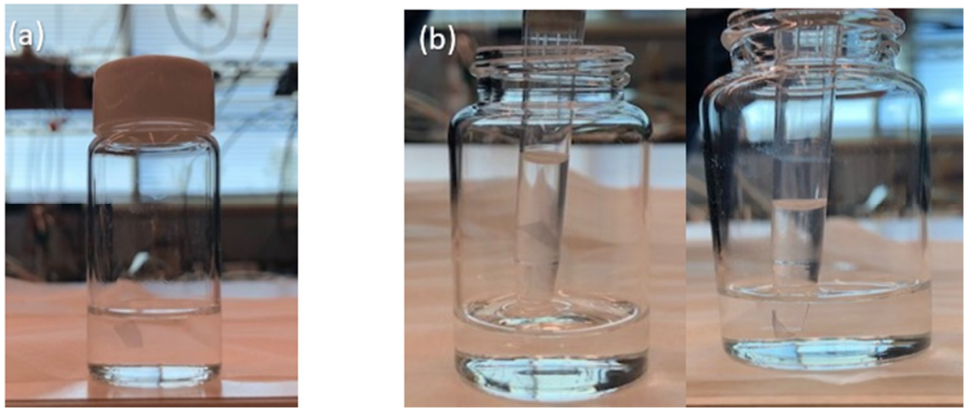

Figure 2.3. Free SWCNT film in ethanol (a). SWCNT film collected in a pipette (b).

2.1.2. CdSe Nanocrystals (CdSe NCs)

CdSe nanocrystals are a semiconductor material with size-dependent optical and electronic properties. In general, CdSe nanocrystals have been implemented in a wide range of applications including solar cells, [58] light-emitting diodes, [59] and fluorescent tagging. However, we used the CdSe nanocrystals (CdSe NCs) as a mechanical stabilizer on SWCNT films by dip-coating a thin layer of CdSe nanocrystals (CdSe NCs). We used around 0.04 g of colloidal CdSe NCs scattered in 0.7 g toluene,or a concentration of 5.5%.A branson 3510 Ultrasonic Cleaner was used to blend NCs with toluene, applied for 7 minutes.

2.1.3. Polydimethylsiloxane (PDMS)

We used Polydimethylsiloxane (PDMS) (Sylgard 184, Sigma-Aldrich) as a substrate in the experiments. We used a 10:1 ratio of elastomer to crosslinker. For example we mixed 13.86 g of the elastomer with 1.38 g of crosslinker, to get a 2 mm thickness of the PDMS substrate in a 100 mm $\times$ 100 mm mold. Then, we placed the mold under an 80 kPa vacuum for an hour to remove all the air bubbles. The vacuum was then decreased to 40 kPa and the mixture was baked at 90°C for 2 hours. Next, we removed the PDMS cut it into 80 mm $\times$ 20 mm $\times$ 2 mm slabs and cleaned them with DI water and ethanol Figure 2.4. Finally, we secured the PDMS in a strain stage.

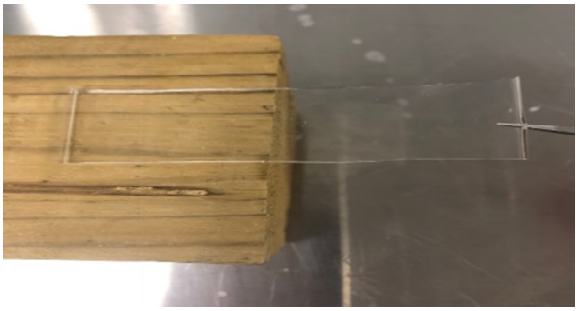

Figure 2.4. Slab of PDMS

2.1.4. Polyacrylamide (PAM)

We used Polyacrylamide (PAM) in our experiment. Polyacrylamide (IUPAC poly(2-propenamide) or poly(1-carbamoylethylene), abbreviated as PAM) is a water-soluble polymer that consists of acrylamide subunits (-CH2CHCONH2-). It increases the viscosity of water and facilitates the flocculation of particles present in water. We prepared the PAM before the experiment for one day to make sure all the granules of the (PAM) dissolved in the DI water. The chemical formula of polyacrylamide is:

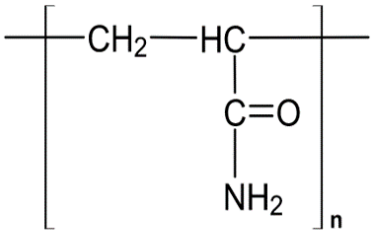

In a typical experiment, we mixed 0.034 g of PAM with 4000 μl of deionized water. Finally, we shook the mixture by hand for 20 minutes as shown in Figure 2.5 (a). We cleaned a rectangular silicon (Si) slide with a length of 20 mm and a width of 5 mm and made up a thin layer of PAM using around 25 μl of the solution on the silicon Figure 2.5 (b).

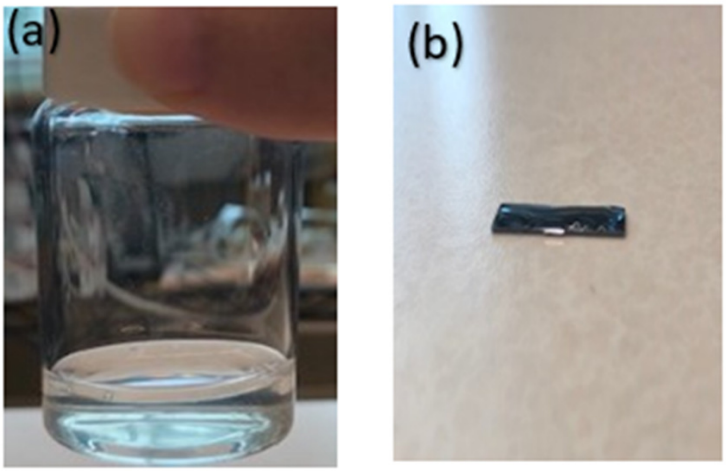

Figure 2.5. PAM was shaken by hand(a). A thin layer of (PAM) on silicon (b).

2.2. SWCNT/ CdSe NC Bilayers

2.2.1. On Polyacrylamide (PDMS)

After the thin layer of PAM had dried on the silicon, we deposited a SWCNT film with a typical length of 10 mm and a width of 2.5 mm above the thin layer of PAM. We deposited the film near the edge because this makes it easier to release the film. Also, it makes it easier to dip the bilayer film into the colloidal CdSe solution. After the SWCNT had dried, we gently dipped the SWCNT film in the dilute CdSe colloidal nanocrystal solution to produce a sharp interface between the pure SWCNT film (without CdSe NCs) and the SWCNT bilayer (with CdSe NCs). We left it in the vacuum for four hours to make sure all the toluene evaporated. With tweezers, we gently placed it in a bath of DI water for 5 hours to dissolve the PAM and free the SWCNT film on the surface of the water. Next, we cleaned a rectangular PDMS substrate installed the PDMS on a strain stage, and applied 15% pre-strain. Then, we made a droplet of DI water on the PDMS. With a piece of silicon, we took the free SWCNT film from the water surface and transferred it to the droplet on the PDMS slide. We deposited the SWCNT film in the DI water droplet to make it easier for us to flatten the film using a pipette. By blowing air from the pipette to generate thrust, we moved the film to the middle on the PDMS and waited for the DI water to evaporate. After the SWCNT film had dried on the PDMS, we released the prestrain in the PDMS using a micrometer to achieve (2, 4, 6, 8, 10, 12)% strain and we took images at each strain with an optical microscope (OLYMPUS TH4-100). We repeated the steps for three different thicknesses: 40, 30, and 10 nm.

2.2.2. On Silicon for Atomic Force Microscope

We did the same process, and we transferred the SWCNT film onto clean silicon to measure the thickness of the SWCNT nanocrystal bilayer using AFM. We cleaned small silicon rectangles and deposited the SWCNT film, half of which is coated by CdSe colloidal nanocrystal. Then, we placed the silicon under a vacuum for 50 minutes to make sure that the SWCNT film was-well-adhered to the silicon. We repeated the steps for three different thicknesses: 40, 30, and 10 nm. To measure the film thickness, we used a Veeco DI-3100 atomic force microscope (AFM) operated in tapping mode with an NT-MDT.FMG01 probe and 10 nm radius tip. For each film, we measured three different spots.

2.3. Tensile Tester

We used an Instron 5545 Tensile Tester with a 100 N load cell to define the Young modulus of the PDMS. The Young modulus was calculated from the slope of the linear (small strain) part of the stress vs. strain curve. After each wrinkling experiment, we calculated the Young modulus for all values in the range of $1.4 < \mathrm{E}_s < 2.5$ MPa [45].

3. RESULTS AND DISCUSSIONS

In the previous experiments, the effectiveness of NCs as mechanical stabilizers on a variety of SWCNT films was investigated by depositing a monolayer of CdSe nanocrystals (CdSe NCs) in a zero-strain (SWCNT perspective) prestretched configuration. A Langmuir-Blodgett (LB) method was used to collect the CdSe NCs on a SWCNT film adhered to pre-stretched PDMS. The measurements indicated a nearly two-fold enhancement in Young's modulus of ultra-thin films associated with the presence of a monolayer of nanocrystals, as shown Figure 3.1 (a,b,c) [45]. Also, step-height was found to be associated with a jump in thickness at such an interface with an average value of $\Delta h = (2.65 \pm 0.25)$ nm Figure 3.1 (d) . The TEM image of a SWCNT film and a SWCNT/NC bilayer interface (20 nm scale) can be see in Figure 3.1 (e) [45].

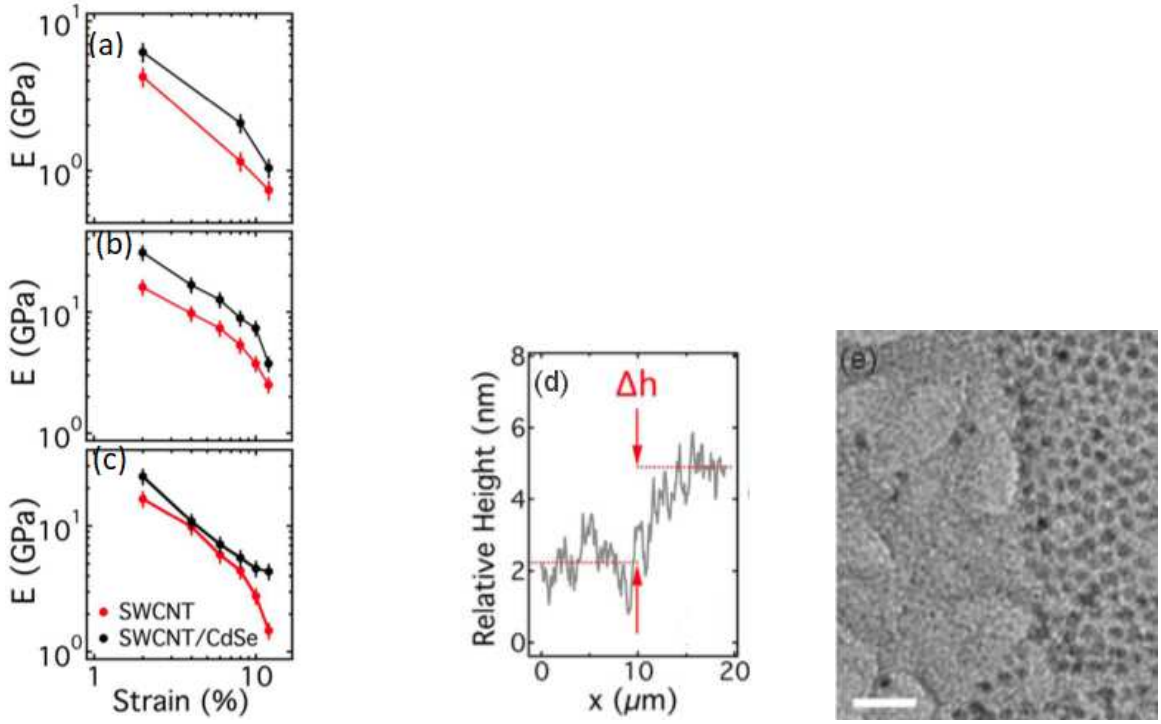

Figure 3.1. (a,b,c) A comparison of measured film moduli both with and without NC for (a) h = 13 nm, (b) h = 17 nm, and (c) h = 40 nm. (d) Mean step height from SWCNT to NC based on the AFM data in panel. (e) TEM image of a NC film edge on an underlying SWCNT film (20 nm scale) [45].

In this experiment, we used the dip-coating method for SWCNT films with CdSe NC. The CdSe colloidal nanocrystals form a sharp interface between pure SWCNT and SWCNT/ CdSe NC bilayer. Figure 3.2 shows the steps of the dip-coating method of making SWCNT and SWCNT-CdSe NCs bilayers.

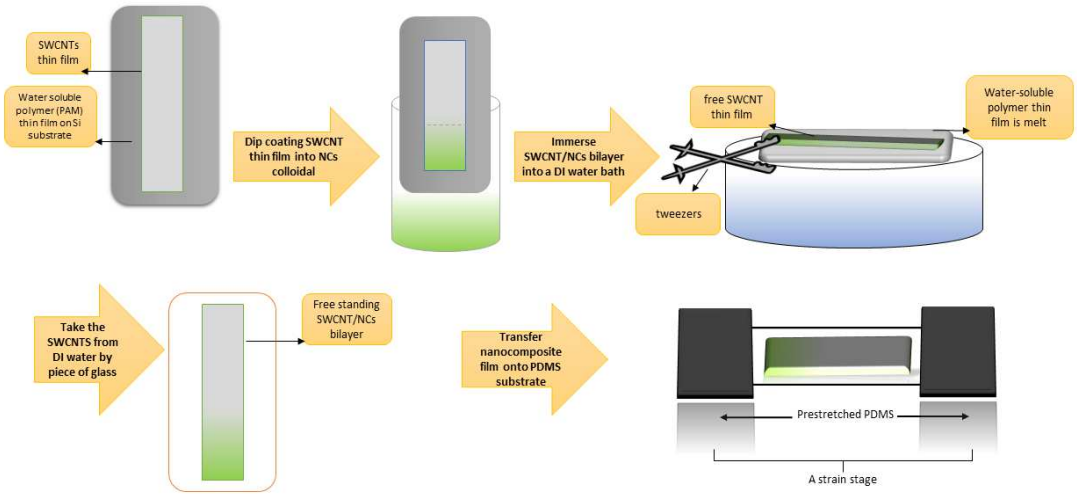

Figure 3.2. The dip-coating method of making SWCNT and SWCNT-CdSe NC bilayers.

Photoluminescence microscopy was used to determine the position of the interface between pure SWCNT and SWCNT/ CdSe NCs bilayer, as shown in Figure 3.3. Also, the wrinkling approach was used to examine the mechanical properties of the hybrid SWCNT/CdSe NCs bilayers.

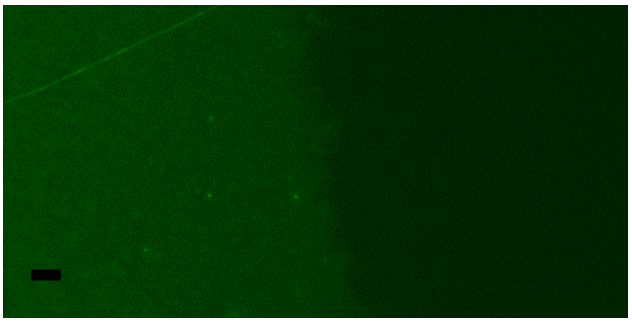

Figure 3.3. PL microscopy image of the sharp interface between SWCNT and SWCNT-CdSe NC bilayer (15 μm scale, $h = 10$ nm).

The fundamental wrinkling mode can easily be distinguished from folds, wrinkles, and ridges, which are all oriented perpendicular to the direction of the applied strain. To count the fundamental wrinkling wavelength λ of each image for the three different thicknesses, we used two approaches: first, we directly measured the distance between each fundamental wrinkle for an ensemble of images. Second, strain (x) projections of the two-point correlation function c($\mathbf{r}$) were digitally computed from grayscale refection optical micrographs. A comparison of this length-scale with the position of the first nearest peak in c(x) is shown in Figure 1.6. In some cases, we had to account for double or quadruple the wavelength because the topography was dominated ridges or folds. As we found, the wrinkling of the SWCNT/ CdSe NC bilayers was different from that of pure SWCNT, as shown in Figure 3.4 (a,b). The change in wrinkling behavior was related to the presence of a CdSe NC monolayer Figure 3.4 (c). Also, the AFM amplitude confirmed that the bilayer had fewer wrinkles in comparison to the pristine SWCNT films, as shown Figure 3.4 (d). The wrinkling wavelength of the bilayer was higher than that of the pristine SWCNT without a significant change in the thickness as shown in the table (3.1).

Table 3.1. Thicknesses of SWCNT-CdSe NC bilayers. The first row is pristine SWCNT and the second row is SWCNT/NC bilayer.

Layer	10 nm experiment	30 nm experiment	40 nm experiment
SWCNT	15.3 nm	30 nm	40 nm
SWCNT/NCs	16.5 nm	30.5 nm	40.7 nm

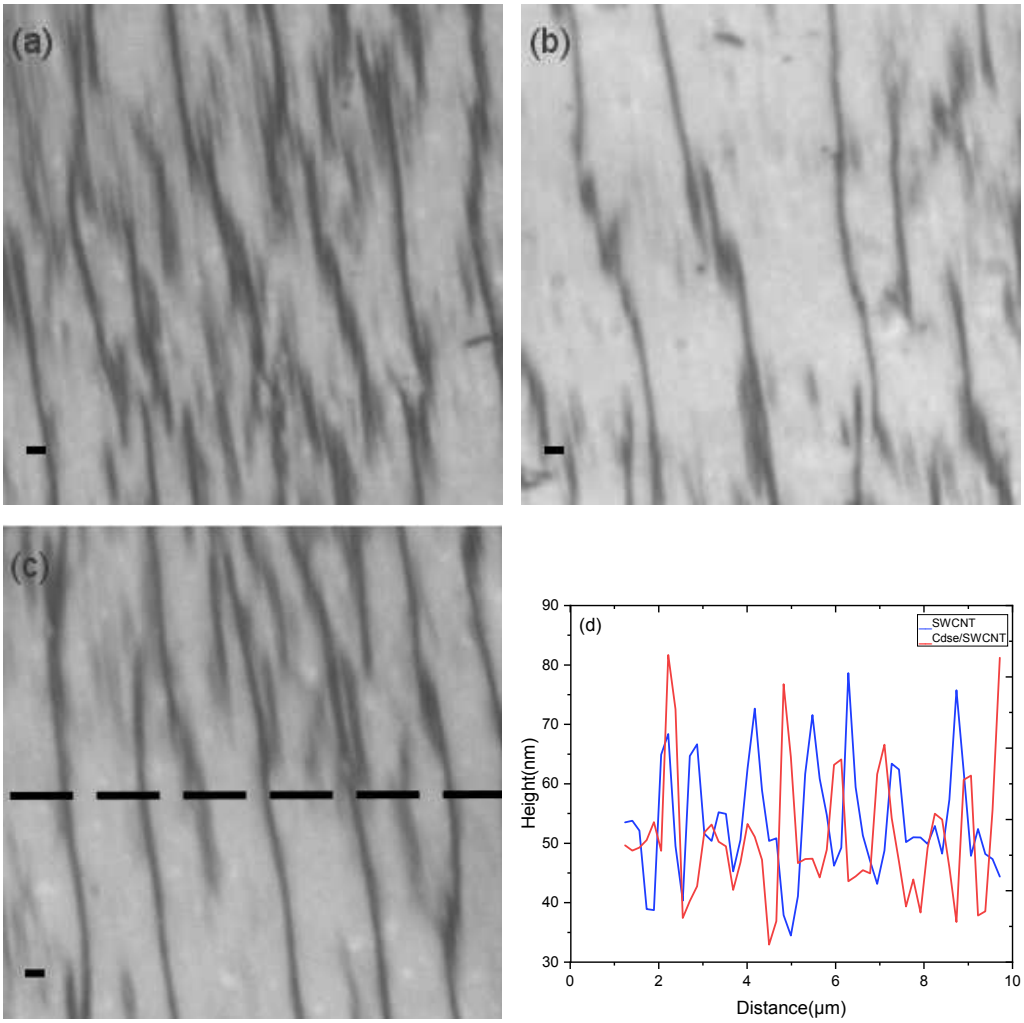

Figure 3.4. (a) Reflection optical micrograph of the wrinkling of a SWCNT film (10 μm scale, $h = 40$ nm, 6% strain). (b) Reflection optical micrograph of the wrinkling of a SWCNT-CdSe NC bilayer (10 μm scale, $h = 40$ nm, 6% strain). (c) Reflection optical micrograph of the wrinkling of SWCNT and SWCNT-CdSe NC bilayer interface (10 μm scale, $h = 40$ nm, 6% strain). (d) AFM wrinkling amplitudes of SWCNT and SWCNT-NC bilayer ($h = 30$ nm).

By using the measured wrinkling length scale and the measured thickness, we applied the strain-induced elastic buckling instability equation (1.1) to measure the Young modulus for dip-coated CdSe NC films. As a result, there was an enhancement in the elasticity of the film for SWCNT films coated with CdSe NCs. The CdSe NC layer enhanced the Young's modulus of the SWCNT films by roughly two-fold Figure 3.5 (a,b,c). In addition, we found an AFM step-height

associated with a jump in thickness at such an interface with an average value of $\Delta h = (2.65 \pm 0.25)$ nm Figure 3.5 (d).

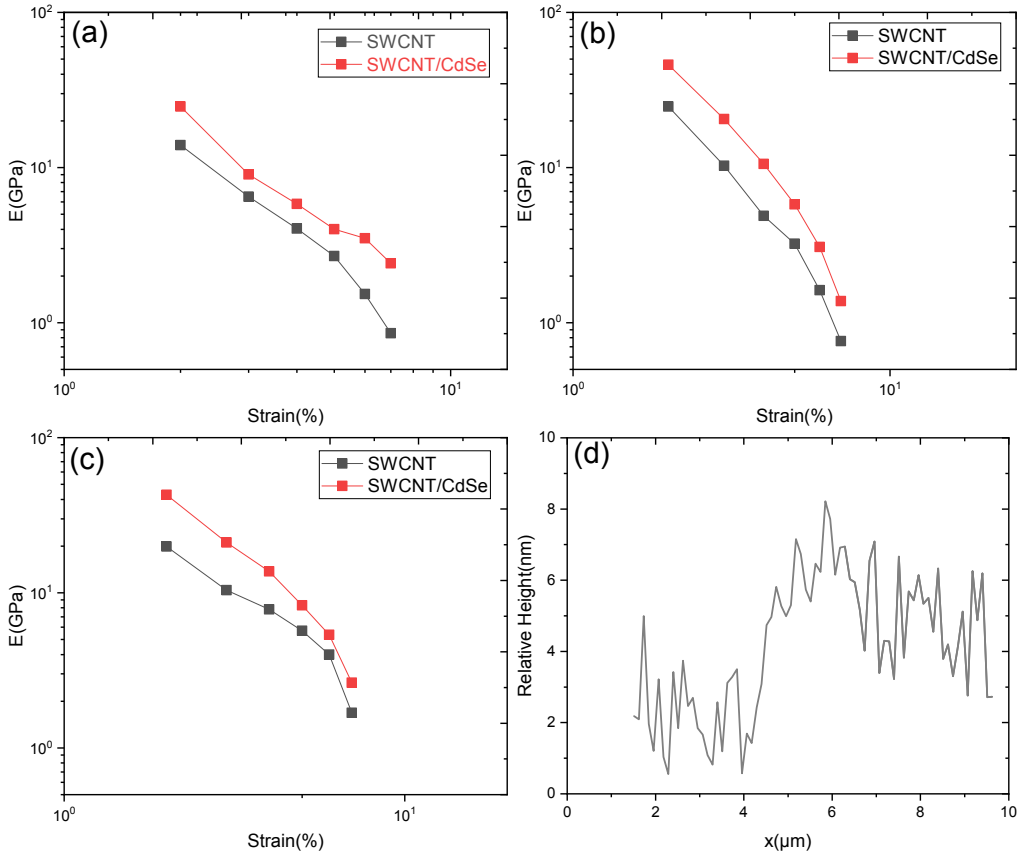

Figure 3.5. A comparison of measured film modulus both with and without NCs for (a) $h = 40$ nm, (b) $h = 30$ nm, and (c) $h = 10$ nm. (d) Mean step height from SWCNT to NC based on the AFM data $h = 40$ nm.

4. CONCLUSION

In conclusion, we have used a strain-induced wrinkling approach to study the mechanical behavior of SWCNT /nanocrystal bilayer films, which were created through dip-coating a SWCNT film in CdSe NC solutions and-deposited on pre-stretched elastic PDMS substrates. Our results have indicated a roughly two-fold enhancement in the Young's modulus of thin films correlated with the presence of a monolayer of nanocrystals. We get enhanced mechanical properties through dip-coated films that have been assembled from hybrid organic and inorganic components, such as SWCNT and colloidal nanocrystals, without the need for chemical modification. Based on our results, we have demonstrated the optimum layer thickness of CdSe NCs for enhanced mechanical behavior for SWCNT films. Our dip coating approach with CdSe NCs gave findings similar to previous work, where elasticity enhancement was found in ultrathin SWCNT films coated with CdSe NCs and spray-coated SiNCs. We believe these results will have useful implications for controlling the rigidity and the strength of nanosheets, including flexible electronic devices.

5. OUTLOOK

Since the discovery of size-dependent electronic properties in nanometer-sized crystals of semiconductors, their characterization, synthesis, and applications have developed a significant fraction of the technologies [60]. So, silicon nanocrystals (SiNCs) have attracted considerable attention for some applications, such as solar cells and LEDs, due to their low toxicity compared to other quantum dots, such as CdSe nanocrystals [61]. Since we can reduce the size of Si materials below the exciton Bohr radius, confinement-induced eligible photoluminescence and other optical properties can be achieved [62]. NDSU has the facilities and state of the art equipment to carry out synthesis, characterization, and device fabrication experiments using silicon nanocrystals using a non-thermal plasma method with a liquid silane precursor. These readily available and high-quality SiNCs are attractive fillers for use in making hybrid SWCNT/SiNC films with potentially useful characteristics. We have demonstrated the viability of Langmuir-Blodgett, spray coating, and now dip-coating approaches for the engineering of these bilayer structures.

REFERENCES

[1] Jupiter Hu. Overview of flexible electronics from itri's viewpoint. In *2010 28th VLSI Test Symposium (VTS)*, pages 84–84. IEEE, 2010.

[2] William S Wong and Alberto Salleo. *Flexible electronics: materials and applications*, volume 11. Springer Science & Business Media, 2009.

[3] Nadja Straue, Martin Rauscher, Martina Dressler, and Andreas Roosen. Tape casting of ito green tapes for flexible electroluminescent lamps. *Journal of the American Ceramic Society*, 95(2):684–689, 2012.

[4] D Purves, GJ Augustine, D Fitzpatrick, WC Hall, AS LaMantia, JO McNamara, and SM Willams. The vestibular system. *Neuroscience. Sunderland, MA: Sinauer Associates, Inc*, pages 343–362, 2008.

[5] Erik T Thostenson, Zhifeng Ren, and Tsu-Wei Chou. Advances in the science and technology of carbon nanotubes and their composites: a review. *Composites science and technology*, 61(13):1899–1912, 2001.

[6] Mohammad Moniruzzaman and Karen I Winey. Polymer nanocomposites containing carbon nanotubes. *Macromolecules*, 39(16):5194–5205, 2006.

[7] Yoichi Murakami, Yuhei Miyauchi, Shohei Chiashi, and Shigeo Maruyama. Direct synthesis of high-quality single-walled carbon nanotubes on silicon and quartz substrates. *Chemical Physics Letters*, 377(1-2):49–54, 2003.

[8] Ekta Singh, Richa Srivastava, Utkarsh Kumar, and A Katheria. Carbon nanotube: A review on introduction, fabrication techniques and optical applications. *Nanoscience and Nanotechnology*, 4(4):120–126, 2017.

[9] Thomas Belin and Florence Epron. Characterization methods of carbon nanotubes: a review. *Materials Science and Engineering: B*, 119(2):105–118, 2005.

[10] Shekhar Subramoney. Novel nanocarbons—structure, properties, and potential applications. *Advanced Materials*, 10(15):1157–1171, 1998.

[11] TW Ebbesen and PM Ajayan. Large-scale synthesis of carbon nanotubes. *Nature*, 358(6383):220, 1992.

[12] László Péter Biró, Carlos A Bernardo, GG Tibbetts, and Ph Lambin. *Carbon filaments and nanotubes: common origins, differing applications?*, volume 372. Springer Science & Business Media, 2012.

[13] Catherine Journet, WK Maser, Patrick Bernier, Annick Loiseau, M Lamy de La Chapelle, dl S Lefrant, Philippe Deniard, R Lee, and JE Fischer. Large-scale production of single-walled carbon nanotubes by the electric-arc technique. *Nature*, 388(6644):756, 1997.

[14] Ting Guo, Pavel Nikolaev, Andrew G Rinzler, David Tomanek, Daniel T Colbert, and Richard E Smalley. Self-assembly of tubular fullerenes. *The Journal of Physical Chemistry*, 99(27):10694–10697, 1995.

[15] Jason H Hafner, Michael J Bronikowski, Bobak R Azamian, Pavel Nikolaev, Andrew G Rinzler, Daniel T Colbert, Ken A Smith, and Richard E Smalley. Catalytic growth of single-wall carbon nanotubes from metal particles. *Chemical Physics Letters*, 296(1-2):195–202, 1998.

[16] Ting Guo, Pavel Nikolaev, Andreas Thess, Daniel T Colbert, and Richard E Smalley. Catalytic growth of single-walled manotubes by laser vaporization. *Chemical physics letters*, 243(1-2):49–54, 1995.

[17] M Yudasaka, R Yamada, N Sensui, T Wilkins, T Ichihashi, and S Iijima. Mechanism of the effect of nico, ni and co catalysts on the yield of single-wall carbon nanotubes formed by pulsed nd: Yag laser ablation. *The Journal of Physical Chemistry B*, 103(30):6224–6229, 1999.

[18] Minfang Zhang, Masako Yudasaka, and Sumio Iijima. Single-wall carbon nanotubes: a high yield of tubes through laser ablation of a crude-tube target. *Chemical physics letters*, 336(3-4):196–200, 2001.

[19] H Kataura, Y Kumazawa, Y Maniwa, Y Ohtsuka, R Sen, S Suzuki, and Y Achiba. Diameter control of single-walled carbon nanotubes. *Carbon*, 38(11-12):1691–1697, 2000.

[20] Daisuke Nishide, H Kataura, S Suzuki, K Tsukagoshi, Y Aoyagi, and Y Achiba. High-yield production of single-wall carbon nanotubes in nitrogen gas. *Chemical Physics Letters*, 372(1-2):45–50, 2003.

[21] M Yudasaka, T Komatsu, T Ichihashi, Y Achiba, and S Iijima. Pressure dependence of the structures of carbonaceous deposits formed by laser ablation on targets composed of carbon, nickel, and cobalt. *The Journal of Physical Chemistry B*, 102(25):4892–4896, 1998.

[22] AA Gorbunov, R Friedlein, O Jost, MS Golden, J Fink, and W Pompe. Gas-dynamic consideration of the laser evaporation synthesis of single-wall carbon nanotubes. *Applied Physics A*, 69(1):S593–S596, 1999.

[23] N Braidy, MA El Khakani, and GA Botton. Effect of laser intensity on yield and physical characteristics of single wall carbon nanotubes produced by the nd: Yag laser vaporization method. *Carbon*, 40(15):2835–2842, 2002.

[24] F Kokai, K Takahashi, M Yudasaka, R Yamada, T Ichihashi, and S Iijima. Growth dynamics of single-wall carbon nanotubes synthesized by co2 laser vaporization. *The Journal of Physical Chemistry B*, 103(21):4346–4351, 1999.

[25] Shunji Bandow, S Asaka, Y Saito, AM Rao, L Grigorian, Eklund Richter, and PC Eklund. Effect of the growth temperature on the diameter distribution and chirality of single-wall carbon nanotubes. *Physical Review Letters*, 80(17):3779, 1998.

[26] AC Dillon, PA Parilla, JL Alleman, JD Perkins, and MJ Heben. Controlling single-wall nanotube diameters with variation in laser pulse power. *Chemical Physics Letters*, 316(1-2):13–18, 2000.

[27] Masako Yudasaka, Toshinari Ichihashi, Toshiki Komatsu, and Sumio Iijima. Single-wall carbon nanotubes formed by a single laser-beam pulse. *Chemical physics letters*, 299(1):91–96, 1999.

[28] Haiyan Zhang, Yu Ding, Chunyan Wu, Yimin Chen, Yanjuan Zhu, Yanyang He, and Shao Zhong. The effect of laser power on the formation of carbon nanotubes prepared in co2 continuous wave laser ablation at room temperature. *Physica B: Condensed Matter*, 325:224–229, 2003.

[29] Susan B Sinnott and Rodney Andrews. Carbon nanotubes: synthesis, properties, and applications. *Critical Reviews in Solid State and Materials Sciences*, 26(3):145–249, 2001.

[30] M José-Yacamán, M Miki-Yoshida, L Rendon, and JG Santiesteban. Catalytic growth of carbon microtubules with fullerene structure. *Applied physics letters*, 62(6):657–659, 1993.

[31] Jin Won Seo, A Magrez, M Milas, Kyumin Lee, V Lukovac, and L Forro. Catalytically grown carbon nanotubes: from synthesis to toxicity. *Journal of Physics D: Applied Physics*, 40(6):R109, 2007.

[32] Kenneth BK Teo, Charanjeet Singh, Manish Chhowalla, and William I Milne. Catalytic synthesis of carbon nanotubes and nanofibers. *Encyclopedia of nanoscience and nanotechnology*, 10(1), 2003.

[33] Catherine Journet and P Bernier. Production of carbon nanotubes. *Applied physics A: Materials science & processing*, 67(1):1–9, 1998.

[34] Seunghun Hong and Sung Myung. Nanotube electronics: A flexible approach to mobility. *Nature nanotechnology*, 2(4):207, 2007.

[35] Michael J O'connell. *Carbon nanotubes: properties and applications*. CRC press, 2006.

[36] Min-Feng Yu, Oleg Lourie, Mark J Dyer, Katerina Moloni, Thomas F Kelly, and Rodney S Ruoff. Strength and breaking mechanism of multiwalled carbon nanotubes under tensile load. *Science*, 287(5453):637–640, 2000.

[37] Teri Wang Odom, Jin-Lin Huang, Philip Kim, and Charles M Lieber. Structure and electronic properties of carbon nanotubes, 2000.

[38] Louis E Brus. Electron–electron and electron-hole interactions in small semiconductor crystallites: The size dependence of the lowest excited electronic state. *The Journal of chemical physics*, 80(9):4403–4409, 1984.

[39] Moungi G Bawendi, Michael L Steigerwald, and Louis E Brus. The quantum mechanics of larger semiconductor clusters (" quantum dots"). *Annual Review of Physical Chemistry*, 41(1):477–496, 1990.

[40] A Paul Alivisatos. Perspectives on the physical chemistry of semiconductor nanocrystals. *The Journal of Physical Chemistry*, 100(31):13226–13239, 1996.

[41] Chung-Lun Wu and Gong-Ru Lin. Inhomogeneous linewidth broadening and radiative lifetime dispersion of size dependent direct bandgap radiation in si quantum dot. *AIP Advances*, 2(4):042162, 2012.

[42] V Alex, S Finkbeiner, and J Weber. Temperature dependence of the indirect energy gap in crystalline silicon. *Journal of Applied Physics*, 79(9):6943–6946, 1996.

[43] Andrew M Smith and Shuming Nie. Semiconductor nanocrystals: structure, properties, and band gap engineering. *Accounts of chemical research*, 43(2):190–200, 2009.

[44] Kashmiri Lal Mittal. *Adhesion measurement of films and coatings*, volume 640. VSP, 1995.

[45] Meshal Alzaid, Joseph Roth, Yuezhou Wang, Eid Almutairi, Samuel L Brown, Traian Dumitrica, and Erik K Hobbie. Enhancing the elasticity of ultrathin single-wall carbon nanotube films with colloidal nanocrystals. *Langmuir*, 33(32):7889–7895, 2017.

[46] Yuezhou Wang, Grigorii Drozdov, Erik K Hobbie, and Traian Dumitrica. Excluded volume approach for ultrathin carbon nanotube network stabilization: A mesoscopic distinct element method study. *ACS applied materials & interfaces*, 9(15):13611–13618, 2017.

[47] Dahl-Young Khang, John A Rogers, and Hong H Lee. Mechanical buckling: mechanics, metrology, and stretchable electronics. *Advanced Functional Materials*, 19(10):1526–1536, 2009.

[48] Erik K Hobbie, Daneesh O Simien, Jeffrey A Fagan, JiYeon Huh, Jun Y Chung, Steven D Hudson, Jan Obrzut, Jack F Douglas, and Christopher M Stafford. Wrinkling and strain softening in single-wall carbon nanotube membranes. *Physical review letters*, 104(12):125505, 2010.

[49] Adam J Nolte, Robert E Cohen, and Michael F Rubner. A two-plate buckling technique for thin film modulus measurements: applications to polyelectrolyte multilayers. *Macromolecules*, 39(14):4841–4847, 2006.

[50] Christopher M Stafford, Christopher Harrison, Kathryn L Beers, Alamgir Karim, Eric J Amis, Mark R VanLandingham, Ho-Cheol Kim, Willi Volksen, Robert D Miller, and Eva E Simonyi. A buckling-based metrology for measuring the elastic moduli of polymeric thin films. *Nature materials*, 3(8):545, 2004.

[51] Dahl-Young Khang, Jianliang Xiao, Coskun Kocabas, Scott MacLaren, Tony Banks, Hanqing Jiang, Yonggang Y Huang, and John A Rogers. Molecular scale buckling mechanics in individual aligned single-wall carbon nanotubes on elastomeric substrates. *Nano letters*, 8(1):124–130, 2008.

[52] John M Harris, Ganjigunte R Swathi Iyer, Anna K Bernhardt, Ji Yeon Huh, Steven D Hudson, Jeffrey A Fagan, and Erik K Hobbie. Electronic durability of flexible transparent films from type-specific single-wall carbon nanotubes. *ACS nano*, 6(1):881–887, 2011.

[53] Matthew R Semler, John M Harris, Andrew B Croll, and Erik K Hobbie. Localization and length-scale doubling in disordered films on soft substrates. *Physical Review E*, 88(3):032409, 2013.

[54] Christopher M Stafford, Shu Guo, Christopher Harrison, and Martin YM Chiang. Combinatorial and high-throughput measurements of the modulus of thin polymer films. *Review of Scientific Instruments*, 76(6):062207, 2005.

[55] Eid Almutairi, Meshal Alzaid, Abu Md Niamul Taufique, Matthew R Semler, and Erik K Hobbie. Rigidity of lamellar nanosheets. *Soft matter*, 13(13):2492–2498, 2017.

[56] Christopher M Stafford, Bryan D Vogt, Christopher Harrison, Duangrut Julthongpiput, and Rui Huang. Elastic moduli of ultrathin amorphous polymer films. *Macromolecules*, 39(15):5095–5099, 2006.

[57] Erik K Hobbie, Thomas Ihle, John M Harris, and Matthew R Semler. Empirical evaluation of attractive van der waals potentials for type-purified single-walled carbon nanotubes. *Physical review B*, 85(24):245439, 2012.

[58] István Robel, Vaidyanathan Subramanian, Masaru Kuno, and Prashant V Kamat. Quantum dot solar cells. harvesting light energy with cdse nanocrystals molecularly linked to mesoscopic tio2 films. *Journal of the American Chemical Society*, 128(7):2385–2393, 2006.

[59] VL Colvin, MC Schlamp, and A Paul Alivisatos. Light-emitting diodes made from cadmium selenide nanocrystals and a semiconducting polymer. *Nature*, 370(6488):354, 1994.

[60] Uwe R Kortshagen, R Mohan Sankaran, Rui N Pereira, Steven L Girshick, Jeslin J Wu, and Eray S Aydil. Nonthermal plasma synthesis of nanocrystals: fundamental principles, materials, and applications. *Chemical reviews*, 116(18):11061–11127, 2016.

[61] Jianwei Liu, Folarin Erogbogbo, Ken-Tye Yong, Ling Ye, Jing Liu, Rui Hu, Hongyan Chen, Yazhuo Hu, Yi Yang, Jinghui Yang, et al. Assessing clinical prospects of silicon quantum dots: studies in mice and monkeys. *ACS nano*, 7(8):7303–7310, 2013.

[62] Abe D Yoffe. Low-dimensional systems: quantum size effects and electronic properties of semiconductor microcrystallites (zero-dimensional systems) and some quasi-two-dimensional systems. *Advances in Physics*, 42(2):173–262, 1993.